Non Local Effects in Window Type Josephson Junctions.

J. G. Caputo [a], N. Flytzanis [b], V. Kurin [b,c],
N. Lazarides [b] and E. Vavalis [d]

[a] Laboratoire de Mathématiques, Institut de Sciences Appliquées
and U.R.A. C.N.R.S. 1378, BP8, 76131 Mont-Saint-Aignan Cedex, France.
[b] Physics Department, University of Crete,71409 Heraklion, Greece.
[c] Institute for Physics of Microstructures,
RAS, Nijny-Novgorod, Russia
[d] Mathematics Department, University of Crete, 71409 Heraklion, Greece and
IACM, FORTH, 71110, Heraklion, Greece.

Abstract

We investigate the influence of the idle region for a thin window junction on its static behaviour which is shown by the characteristic curves of the maximum critical current versus the extenally applied magnetic field. This system reduces to a one dimensional integro-differential equation. The numerical solution of the non-local equation shows that the existence of the idle region introduces a new effective length, which depends on its size. The solution differs considerably from the known sine-Gordon soliton, while the $I_c - H$ curves with inline and overlap current feed change significantly.

Pacs numbers: 74.50.+r, 74.60.Jg, 03.40.Kf, 02.90.+p

1 Introduction

A Josephson junction consists of two superconducting layers (electrodes) separated by a thin oxide layer allowing the tunneling of Cooper pairs and/or quasiparticles. This is a highly nonlinear system, because of the Josephson current - phase relation, which causes localisation of the magnetic flux that penetrates the oxide and the electrodes (within the London penetration depth λ_L). Its electromagnetic properties as an oscillator are described by the well known sine Gordon equation, for the phase difference ϕ of the macroscopic order parameters in each superconductor. For long junctions, where their length exceeds the Josephson penetration depth λ_J, it is known that the sine Gordon equation admits soliton solutions (fluxons). The static and dynamic properties of these fluxons have been studied extensively both theoretically and experimentally [1, 2].

In practice however the technology of fabrication of modern Josephson junctions is such that the top and bottom superconducting films occupy an area larger than the one of the junction itself. This results in a thick insulating region, which is called the idle region, all around the junction area. The idle region or passive region, is a superconductor - insulator - superconductor structure around the junction perimeter, where no tunneling takes place between the electrodes. This method offers a way to avoid problems related to the film edges, like poor barrier quality, altered T_c, or bad coverage. It makes also easier to study geometrical effects in junctions having non traditional shapes. The idle region serves also

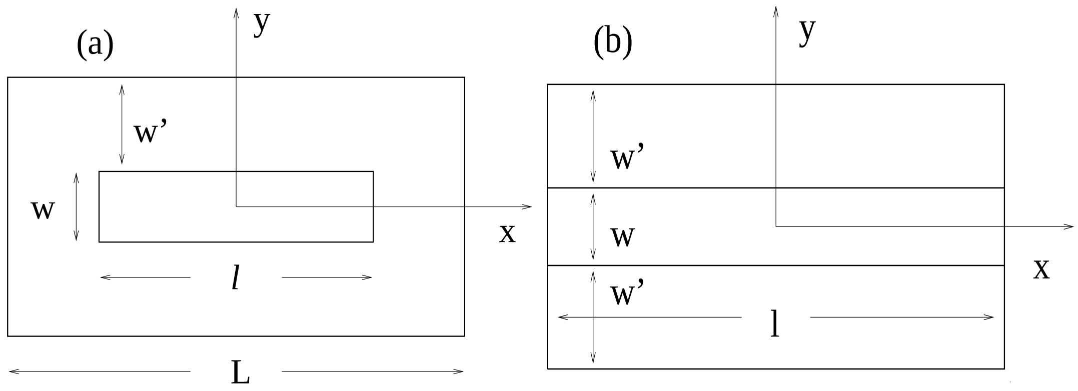

Figure 1: Schematic drawing of: (a) a window junction with inline-overlap boundary conditions; (b)truncation of the device shown in (a), where the longitudinal passive region has been eliminated.

as a cavity to which the oscillator can couple with adjustable impedance mismatch, thus increasing the output power of the device.

The passive region plays an important role in the dynamic and static properties of these window junctions. Various experiments in such structures have been performed [4, 5, 11], revealing interesting phenomena, which are not seen in the usual junctions. For example, a large passive region can lead to the disappearence of the zero field steps, dynamical states corresponding to the shuttling of a soliton inside the window [3]. The static properties of these devices, which are characterised by the maximum critical current I_{max} versus the applied magnetic field H curve, are also strongly affected. As the extension of the idle region w' increases, the I_{max} also increases, until it reaches a limiting value. Also, the critical field H_{c1}, where the current vanishes for the first time, decreases considerably [3, 8]. Another experimental study emphasized the different roles played by a lateral or longitudinal passive region for long junctions [4]. A lateral passive region causes an increase of the velocity of the linear waves in accordance with the result on the dispersion curve obtained by Lee [6, 7], while a longitudinal passive region only acts as a lumped capacitance on both ends of the junction.

We also emphasized the fundamental role of the lateral passive region for window junctions by considering static fluxon solutions [8, 9, 10]. We showed that the fluxon width in such a system is not given by λ_J as in the case of a usual junction, described by the sine-Gordon equation, but by a larger characteristic length of magnetic flux variation λ_{eff}. In Ref.[8] it was also shown that λ_{eff} can be used for a quantitative understanding of the behaviour of I_{max} for a given magnetic field H.

Here we extend this approach by showing that the $I_{max} - H$ curve for both inline and overlap geometries can be accurately described by a one dimensional non-local model of the sine Gordon type, when the junction is sufficiently narrow. In this case, the results are in excellent agreement with the two dimensional calculations.

In section 2 we describe the two dimensional model of two coupled PDEs and its reduction to a one dimensional integro-differential equation of the sine-Gordon type, for a finite length, thin junction, with lateral idle region (Fig. 1b). In section 3 we present some numerical results for this model, and in the last section we discuss those results and give our conclusions.

2 The Finite Long Thin Junction Model.

We consider the case of a finite length window junction as shown in Fig.1b with mixed inline-overlap boundary conditions. The length of the junction and the idle region is l, while the width of the junction and the idle region are w and w', respectively. For our purposes, we can neglect the longitudinal passive region, since this does not contribute to λ_{eff} [8], in accordance with the experiments [4]. We shall also assume a very narrow junction. Going from the design in Fig.1a to this in Fig.1b we neglect the point effects at the tips of the junction which will be clearly present in the case of different surface inductances leading to a discontinuity of the x component of the phase gradient.

The two dimensional system consists of the sine-Gordon equation $\Delta\phi = \sin\phi$ in the window, and the Laplace equation $\Delta\psi = 0$ in the idle region, where ϕ and ψ are the normalized phase differences in the junction and passive region, respectively. These equations are coupled through the continuity conditions for the phase and surface current at the junction-idle region interface, and outside boundary conditions

$$\phi_x|_{x=\pm\frac{l}{2}} = H \pm \frac{\alpha}{2}, \qquad \psi_x|_{x=\pm\frac{l}{2}} = (H \pm \frac{\alpha}{2}), \qquad \psi_y|_{y=\pm(\frac{w}{2}+w')} = \frac{\pm\delta}{2}, \tag{1}$$

where α, δ are the (uniform) current densities and H the (uniform) magnetic field.

The procedure we shall follow consists of solving the Laplace problem in the idle region and subsequently coupling to the equation in the junction. First we transform the Laplace problem to Neumann problem, introducing an appropriate auxiliary function $f(x)$ and the variable $\theta(x, y)$ such that $\theta(x, y) = \psi(x, y) - f(x)$. Now we express the problem in θ:

$$\Delta\theta = -\frac{\alpha}{l} \tag{2}$$

$$\theta_x|_{x=\pm\frac{l}{2}} = 0, \quad \theta_y|_{y=\frac{w}{2}} = \frac{w}{2}I, \quad \theta_y|_{y=\frac{w}{2}+w'} = \frac{\delta}{2}, \tag{3}$$

which can be solved by expanding θ in cosine Fourier series in x:

$$\theta(x, y) = \sum_n \theta_n(y) \cos k_n(x + \frac{l}{2}), \quad \text{where} \quad k_n = \frac{\pi n}{l} \tag{4}$$

where the cosine Fourier component of θ is found to be

$$\theta_n(y) = A_n \cosh k_n(y - \frac{w}{2}) + B_n \sinh k_n(y - \frac{w}{2}) + \frac{\alpha_n}{lk_n^2}, \tag{5}$$

$$\text{with} \qquad A_n = \frac{(\delta_n - wI_n \cosh kw')}{2k_n \sinh k_n w'} \qquad \text{and} \qquad B_n = \frac{wI_n}{2k_n}. \tag{6}$$

I_n is still an undetermined quantity. Its cosine transform, $I(x)$, acts as an overlap current input for the window domain, as can be seen by averaging the static 2-d sine-Gordon equation over y for a narrow width:

$$-\Phi_{xx} + \sin\Phi = \frac{1}{w}[\phi_y]_{-\frac{w}{2}}^{\frac{w}{2}} \equiv I(x), \tag{7}$$

where $\Phi(x)$ is the $y-$averaged phase along the window. From Eqs.(5,6) we express I_n as a function of $\theta_n(\frac{w}{2})$, and by matching the phases at the interface we can get I_n as a function of Φ_n. Replacing $I(x)$ in Eq.(7) yields the non-local equation describing the thin window junction

$$-\Phi_{xx} + \sin\Phi = \frac{\delta}{w} - \frac{2}{w}\sum_n \left(\Phi_n - f_n - \frac{\alpha_n}{lk_n^2}\right) k_n \tanh k_n w' \cos k_n(x + \frac{l}{2}), \tag{8}$$

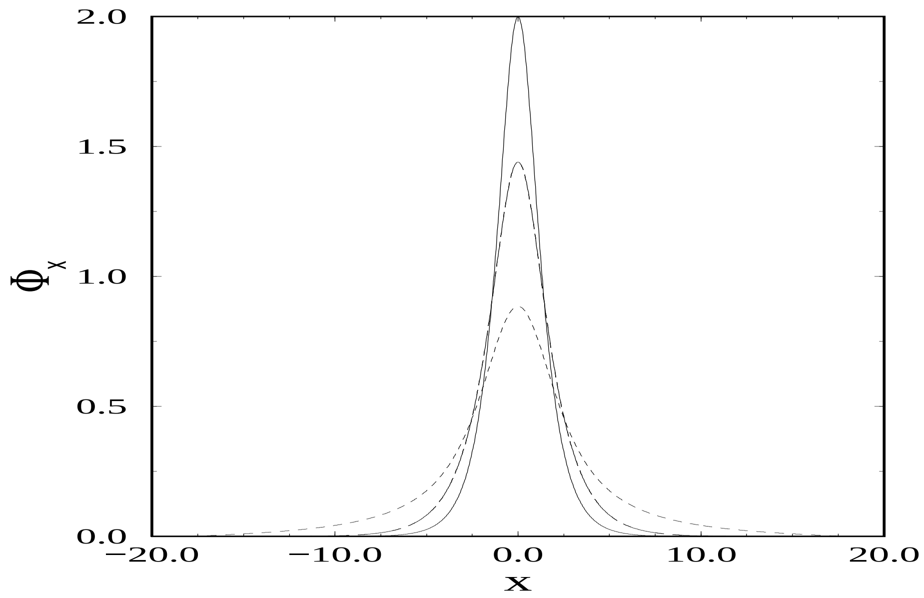

Figure 2: Plot of $\Phi_x(x)$ for a finite length junction with $l = 36$, $w = 1$ and $w' = 0$ (solid line), 2 (long dashes), 5 (short dashes).

with the boundary conditions

$$\Phi_x\left(x = \pm\frac{l}{2}\right) = H \pm \frac{\alpha}{2}.$$

3 Numerical Results.

For the numerical evaluation of the single static fluxon in a finite length junction we can use the cosine Fourier tranform of Eq.(8) with $\delta = 0$. We get a system of highly nonlinear algebraic equations for the cosine Fourier components of $\Phi(x)$, which can be easily solved by a simple iteration scheme:

$$\tilde{\Phi}_k^{(n+1)} = \frac{1}{r + K(k)}\left(r\tilde{\Phi}_k^{(n)} - [sin\Phi^{(n)}]_k\right), \quad n = 0, 1, 2, \cdots, \tag{9}$$

$$\text{where} \quad K(k) = k^2 + \frac{2k}{w}tanh(kw') \tag{10}$$

The subscript "k" denotes the k_n cosine component, with $k_n = \frac{\pi n}{l}$. The factor $r\tilde{\phi_k}$ was added in both sides of the equations to avoid the vanishing of the denominator for $k = 0$ and speed up the convergence. The relaxation parameter r is taken to be $r = 1.5$.

Iterating the previous equation, we get the solution with very high precision within a few iterations. We use a very fine spatial grid, with $N_x = 1025$ points. The cosine Fourier transform is realized using the routine DFCOST from the IMSL/MATH LIB. To check the convergence of our solution we calculate the norm of the difference of subsequent solutions (i.e. $d\Phi_{n+1,n} \equiv \left[\sum_{i=1}^{N_x}(\Phi^{(n+1)} - \Phi^{(n)})^2\right]^{\frac{1}{2}}$) and stop the iteration when $d\Phi_{n+1,n} < 10^{-10}$. The solutions for $w' = 0,\ 0.5,$ and 5.0 are shown if Fig.2.

In order to trace the $I_{max} - H$ curves, we start from the (0,0) point on the $I_{max} - H$ plane with zero initial conditions. Subsequently we increase the current in small steps until the solution does not converge in a certain number of iterations. Then, we go back to the last

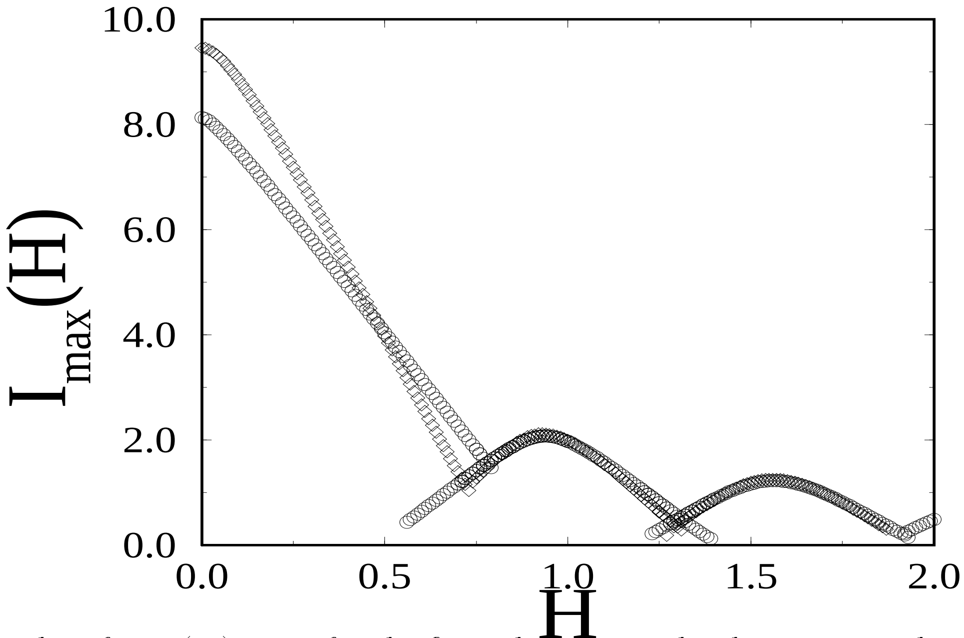

Figure 3: Plot of $I_{max}(H)$ curve for the finite domain non-local junction with inline current feed. The parameters are $l = 10,\ w = 1,\ w' = 2$ (circles), $w' = 5$ (squares).

point where the solution converged and half the current step. This procedure continuous until the step reaches a certain tolerance CTOL. We find empirically that a small CTOL is needed to trace the $I_{max} - H$ branches without problems. Subsequently we increase the magnetic field and follow the same procedure. We performed the calculations for $w' = 2, 5$ with inline current feed ($\delta = 0$), The case with $w' = 0$ which is of course the pure sine Gordon case, has been studied by Owen and Scalapino [12]. It served as a test for the accuracy of our numericall code. We find that for $H = 0$ the numerically calculated value differs from the correct theoretical value $I_{max}(0) = 4$, only by about 0.1%. The $I_{max} - H$ curves for $w' = 2$ and $w' = 5$ are shown in Fig.3.

4 Discussion and Concluding Remarks

There are a few interesting features in those numerical results. First of all, the derivative of the solution Φ_x changes dramatically as w' increases, developing very long tails. The width of Φ_x increases a lot, as well. Also, the zero field critical current increases considerably even for moderate w' values, reaching 95% of its saturation value already for $w' = 5$. On the other hand, the value H_{c1} where the critical current becomes zero for the first time (where a full fluxon enters the junction) decreases considerably when the idle region increases. For very small magnetic fields the first branch of the $I_{max} - H$ curves looses its linearity, as w' increases.

Those features indicate that the classification of a window junction as short or long does not depend on whether $l << 1$ or $l > 1$, like in the pure sine Gordon case, but one has to consider an effective junction legth l/λ_{eff}. Thus, the existence of the idle region introduces a new characteristic length, λ_{eff}, which depends on its size. This means, that even a junction with length $l = 10$ is a short one, if the passive region extension w' is big enough approaching the diffraction-like pattern for $I_{max} - H$. An estimation of the λ_{eff} can be obtained with a variation of a functional with respect to the effective width d of the fluxon (actually it is the free energy of a junction of infinite length), which in the case of zero external current

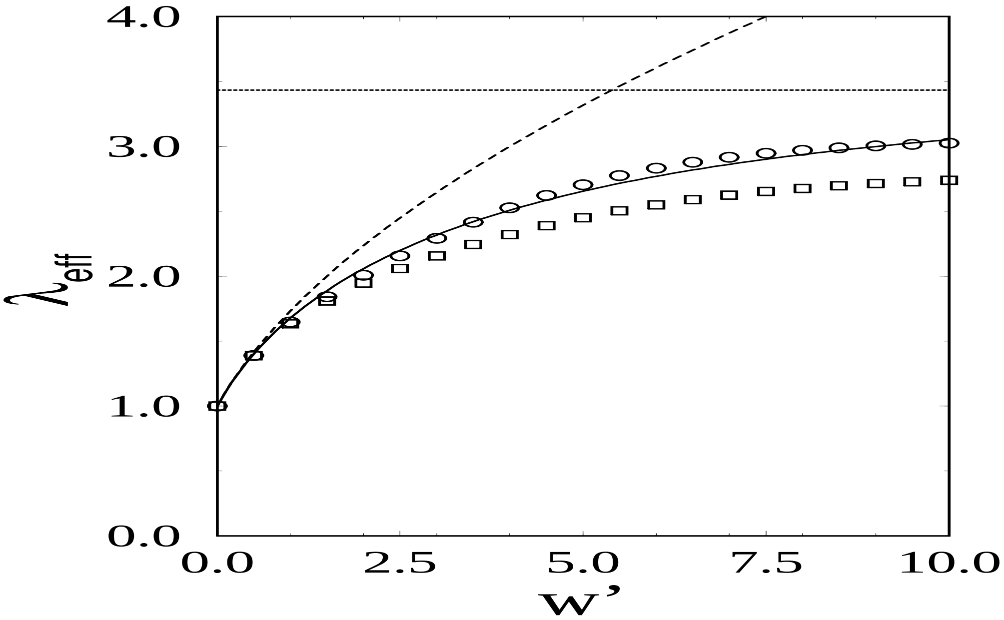

Figure 4: Plot of the fluxon width d vs. the passive region extension w' obtained from: (a) solution of the variational method (solid line); (b) small w' limit (short dashes); (c) Infinite w' limit (long dashes); and (d) numerical solution of Eq.(8) for finite lengths with $l = 12$ (circles) and $l = 15$ (crosses).

$(\delta = \alpha = 0)$ can be written as

$$F = \int_{-\infty}^{+\infty} dx \; (\frac{\Phi_x^2}{2} + 1 - \cos\Phi) - \frac{1}{w}\int_{-\infty}^{+\infty} dx \int_{-\infty}^{+\infty} dx' \Phi_x(x) K(x-x')\Phi_x(x'), \qquad (11)$$

where $K(x-x')$ is the kernel with a Fourier tranform

$$\tilde{K}(k) = \frac{\tanh kw'}{k}.$$

Thus the second term of F can be written by using the convolution theorem as

$$\mathcal{I} = \int_{-\infty}^{+\infty} dx \int_{-\infty}^{+\infty} dx' \Phi_x(x) K(x-x')\Phi_x(x') = \frac{1}{2\pi}\int_{-\infty}^{+\infty} dk \; \tilde{\Phi}_x(-k)\tilde{K}\tilde{\Phi}_x(k). \qquad (12)$$

The calculations are easier if one considers $q(x) \equiv (\Phi_f)_x = \frac{2}{d}\frac{1}{\cosh\frac{x}{d}}$ with its Fourier transform $\tilde{q}(k) = 2\pi \mathrm{sech}\frac{\pi k d}{2}$. Summing all the terms yields the expression for F

$$F\{\Phi_f\} = \frac{4}{d} + 4d + \frac{2\pi}{w}\int_{-\infty}^{+\infty} dk \frac{\tanh kw'}{k}\frac{1}{\cosh^2\frac{\pi k d}{2}}. \qquad (13)$$

Computing the derivative of F with respect to d we obtain

$$\frac{\partial F}{\partial d} = -\frac{4}{d^2} + 4 - \frac{2\pi^2}{w}\int_{-\infty}^{+\infty} dk \tanh kw' \cosh^{-3}\frac{\pi k d}{2}\sinh\frac{\pi k d}{2}. \qquad (14)$$

Equating $\frac{\partial F}{\partial d}$ to zero, and solving the resulting equation numerically, we get d as a function of w'. One can also derive relations for the limiting behaviours of d, for $w' \to 0$ and $w' \to \infty$ [8, 9].

Notice that we used λ_{eff} instead of d in Fig.4. The two quantities are actually the same thing, since it is the width of the fluxon which determines the characteristic length for the

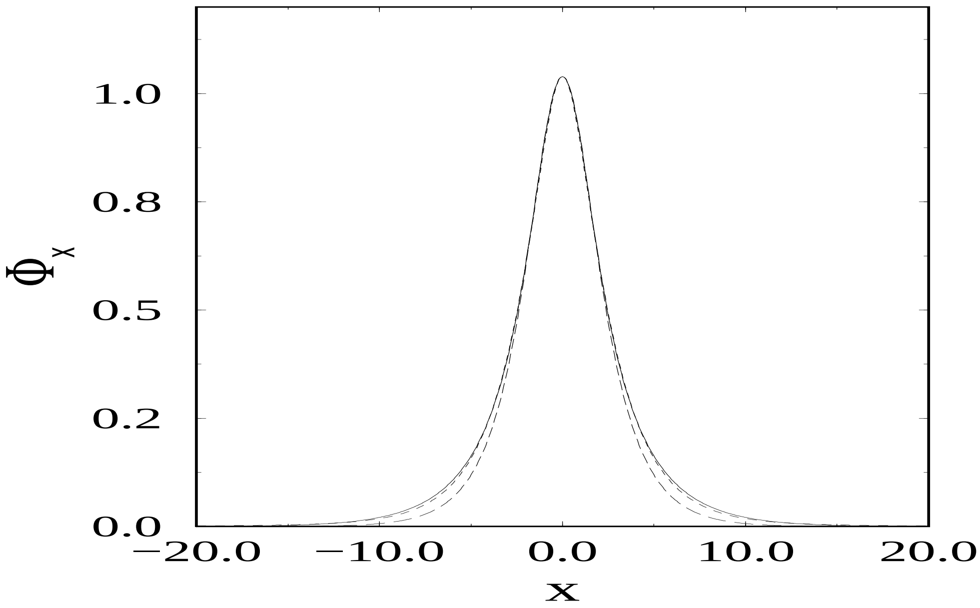

Figure 5: The case $w' = 2$ (solid line) is fitted by a sech-type form (dashed line), and by Eq.(8) with $\alpha = 0.786$, $d_1 = 2.050$, and $d_2 = 1.57$ (short-dashed line).

junction. In Fig.4 we plot the fluxon width obtained from the variational procedure, together with the limiting behaviors, for $w' \to 0$ (short dashed curve) and for $w' \to \infty$ (long dashed curve). It can be seen that the curve for small w' describes well the situation for $w' < 1$, but diverges fast from the variational result for higher w'. The asymptotic value for $w' \to \infty$, which depends only on the width of the window, in this case is $\lambda_{eff} = 3.43$ (where $w' = 1$). In the same figure we present the results obtained by fitting the numerical solution from Eq.(8) to a function of the form $\Phi_x = \frac{2}{d} sech \frac{x}{d}$, for $l = 12$ (circles) and $l = 15$ (squares).

It should be remarked that the width of the fluxon is not a sufficient parameter to characterise the solution since the form of the solution is not of a simple sech−type (for Φ_x) but also has a tail component which becomes more important as you increase the size of the passive region, as it is obvious from Fig.2.

A good fitting of the numerical solutions can be achieved if we use as a trial function a combination of a sine Gordon soliton and an algebraic soliton with the appropriate coefficients:

$$\Phi_x = \alpha \frac{2}{d_1} sech(-\frac{x}{d_1}) + (1-\alpha) \frac{d_2}{x^2 + d_2^2} \qquad (15)$$

In Fig.5 we show the numerical solution $w' = 2$ along with two fittings: one with $\alpha = 1.0$ in Eq.(15) (long dashes), and the other with $\alpha = 0.786$, $d_1 = 2.050$, and $d_2 = 1.570$ (short dashes). The parameters were found by minimizing an appropriate function χ^2, with respect to α and d_1. The third parameter is fixed by the value of the calculated Φ_x, at $x = 0$. In the second case we get a much better fitting.

Apparently, the second term of Eq.(15) has a large contribution in fitting the solution. This contribution increases as w' increases. The values of α for the values of $w' = 0.5, 2.0, 5.0$ are $\alpha = 0.976, 0.786$, and 0.503, respectively.

We should also remark that the same calculations were done for the $I_{max} - H$ curves with the two dimensional model, showing excellent agreement with the one dimensional non-local model, for narrow junctions.

An important physical effect which we have not considered in this study is the difference in the surface inductances between the active and passive regions. In this case the reduction of the uniformly surrounded junction of Fig. 1a to the lateral passive region junction of Fig. 1b is not physically meaningful because this introduces discontinuities of the x derivative of the phase at the interface. In this case the solution has some delta function singularities at each corner of the interface, and this problem cannot be used to understand the uniform window case.

Acknowledgments

Part of this work was supported by an INTAS grant and a PENED grant (No. 2028/1995). V. K. and J. G. C. acknowledge the hospitality of the University of Crete. The visit of J.G.C. was made possible by a grant under the Greek-French collaboration agreement and the visit of V. K. by a grant from the University of Crete.

References

[1] A. Barone and G. Paterno, *Physics and Applications of the Josephson effect*, John Wiley, New York, 1982.

[2] K. Likharev, *Dynamics of Josephson Junctions and Circuits*, Gordon and Breach, New York, 1986.

[3] N. Thyssen, A. V. Ustinov, H. Kohlstedt, J. G. Caputo, S. Pagano, and N. Flytzanis, Proc. of the Intl. Conf. on "Nonlinear Superconducting Devices and High$-T_c$ Materials". Eds. R. D. Parmentier and N. F. Pedersen. Capri, October 8-13, 1994, Italy.

[4] R. Monaco, G. Costabile, and N. Martucciello, *J. Appl. Phys.* **77**, (5) 2073–2080, 1995.

[5] R. Monaco, G. Costabile, and N. Martucciello, Proc. of the Intl. Conf. on "Nonlinear Superconducting Devices and High$-T_c$ Materials". Eds. R. D. Parmentier and N. F. Pedersen. Capri, October 8-13, 1994, Italy.

[6] C. Lee, *IEEE Trans. Applied Superconductivity*, 1:121–125, 1991.

[7] C. Lee and A. Barfknetcht, *IEEE Trans. Applied Superconductivity*, 2:67–73, 1992.

[8] J. G. Caputo, N. Flytzanis and E. Vavalis, *Int. Jour. Mod. Phys.* **C 7**, 191, 1996.

[9] J. G. Caputo, N. Flytzanis, and E. Vavalis, *Int. J. Modern Physics* **C 6**,241, 1995.

[10] J. G. Caputo, N. Flytzanis, and M. Devoret, *Phys. Rev.* **B 50**, 6471, 1994.

[11] P. Barbara, R. Monaco and A. V. Ustinov, *J. Appl. Phys.* **79**, 327, 1996.

[12] C.S. Owen and D.J. Scalapino, *Phys. Rev.* **164**, 538–544, 1967.